Journal of Marine Research, 42, 83–102, 1984

An unstable uniform slab model of the mixed layer as a source of downward propagating near-inertial motion Part 2: Unsteady mean flow

by John Kroll[1]

ABSTRACT

The model of the uniform slab model of the mixed layer which was previously analyzed for stability (Kroll, 1982) is modified to include inertial oscillations in the mean flow. The results reflect the nature of the parallel flow instability produced by the steady component of the mean flow combined with the nature of a parametric instability produced by the oscillating component of the mean flow. This model is much more likely to produce unstable perturbations with a near-inertial frequency than the steady mean model which reinforces the contention that the instability can be a source of vertically propagating inertial oscillations. Also certain frequencies that are integral multiples of the inertial frequency above a near-inertial frequency can be significant in the perturbation. The energy flux associated with these frequencies predominates as the inertial oscillations in the mean flow become significant. This could produce a significant energy flux from the mean flow.

1. Introduction

In Kroll (1982) we looked at the stability of the uniform slab model of the mixed layer, neglecting the inertial oscillations in the mean flow. From here on we will designate that work as (I). In this paper we include these previously neglected inertial oscillations in the mean flow. The resulting model is certainly more realistic than that in (I) since in a real mixed layer the amount of energy in the oscillations is as likely as not to be as great or greater than that in the steady mean.

The solution, as expected, reflects the nature of the parallel flow instability of (I) in combination with a parametric instability of a type similar to those described by Kelly (1965) and Mied (1976) for example. The model is mathematically complicated and its numerical solution is costly. Hence we were not able to explore the nature of the solution as extensively throughout the parameter space as we would have liked.

In (I) we compared two flow scenarios: one where the flowrate increased to a critical value with the depth of the mixed layer essentially fixed and a second where the flowrate was fixed and the depth increased to a critical value. The calculations were done correctly, however, an unrealistically small value of the ratio of the Brunt-Väisälä

1. Department of Mathematical Sciences, Old Dominion University, Norfolk, Virginia, 23508, U.S.A.

to the inertial frequency (N_o/f_o) was used. A value of 40 was mistakenly used rather than 400. Results, using either value, seem qualitatively the same. However, for the more realistic value, the frequency at the critical point tends not to be near-inertial. Hence it seems not as likely as first presumed that the frequency in (I) will be near-inertial. However, we will show that it is much more likely for realistic conditions for this present model. We will not compare the two flow scenarios here because of the large computing cost.

2. The mathematical model

As in (I), we are considering uniform mixed layer slab flow over a continously stratified, infinite depth interior with a stable density jump across the interface. The basic perturbation equations, variables, and parameters are the same as those used in (I) unless otherwise noted. However, inertial oscillations are included in the steady-state flow. Assuming the system is initially at rest, this can be shown to be

$$(u, v) = \frac{\tau_o}{f_o \rho_1 h} \{\sin\theta + \sin(f_o t - \theta), -\cos\theta + \cos(f_o t - \theta)\} \tag{1a}$$

where τ_o is the magnitude of the wind stress, h and ρ_1 the depth and density of the mixed layer respectively, the angle θ is measured from the x-axis. If we assume that our perturbation wave in the stability analysis is in the x-direction, then θ is the angle between the direction of wind and the perturbation wave. It can be shown that in this case v in (1a) enters no further in our analysis. In reality, due to wind shifts and decay, the ratio of the magnitude of steady and oscillating parts of u can vary. Thus for the steady-state velocity we will use

$$u = U_o U(t) = U_o [(1 - \epsilon)\sin\theta + \epsilon \sin(ft - \theta)] \tag{1b}$$

where $0 \leq \epsilon \leq 1$. Thus for $\epsilon = 0$, we have pure transport and for $\epsilon = 1$ we have pure oscillations. The $\epsilon = 0$ case corresponds to the model of (I).

As in the simpler model, there exists an infinite set of stable solutions of the perturbation equations which are independent of the lower layer and which we will neglect. The solutions we are looking for then have velocity independent of z in the mixed layer. Using the perturbation equations and interface conditions at $z = -1$, we obtain the following dimensionless equations after eliminating all variables except eastward velocity, u, pressure, p, and interface displacement, η.

For the mixed layer

$$\tilde{u}_{tt} + 2(ikRU + \sigma k^2)\tilde{u}_t + (f^2 + ikRU_t + (ikRU + \sigma k^2)^2)\tilde{u} = -ik\tilde{p}_{o_t} - ik(ikRU + \sigma k^2)\tilde{p}_o \tag{2a}$$

and

$$u = \frac{-i}{k}\,[\tilde{\eta}_t + ikRU\tilde{\eta}]. \tag{2b}$$

For the stratified ocean beneath

$$(\tilde{P}_{\xi\xi} - \gamma\tilde{P}_\xi)_{tt} + f^2(\tilde{P}_{\xi\xi} - \gamma\tilde{P}_\xi)_t - B_o^2k^2\tilde{P}_t = 0 \tag{3a}$$

and

$$\tilde{\eta}_t = \frac{-1}{B_o^2}\,\tilde{P}_{\xi t}(\xi = 0) \tag{3b}$$

where $(\ ) = (\tilde{\ })e^{ikx}$, $\tilde{P} = \alpha\tilde{\eta} + \tilde{p}$, $\tilde{p}_o$ is the pressure at the interface $z = -1(\xi = 0)$, and $\gamma = B_\xi/B$ is assumed constant as in (I). The nondimensionalization and the dimensionless parameters are the same as for (I). These are summarized in Table 1. It should be noted that $f = 1$ while f_o is the dimensional inertial frequency, and we will assume that the horizontal scale, L, is such that $\sigma = 1$; i.e., $L = \sqrt{\nu_H/f_o}$, as in (I).

Kelly (1965) analyzed the stability of an oscillating Kelvin-Helmholtz flow. His system resulted in a Mathieu equation to be solved. This type of instability is called a parametric instability. In its most elementary form it is the behavior of the pendulum with oscillating length, the trapeze instability described by Orlanski (1973). Our system is much more complicated. If we simplify our system letting $\sigma = \gamma = 0$, we obtain the following system of equations for $N(t)$ and $P(\xi, t)$:

$$N_{tt} + (f^2 + \alpha k^2)N = k^2e^{\phi}P(o, t), \tag{4a}$$

$$N = -\frac{1}{B_o^2}\,e^{\phi}P_\xi(o, t), \text{ and} \tag{4b}$$

$$P_{\xi\xi tt} + f^2P_{\xi\xi} - B_o^2k^2P = 0, \text{ where} \tag{4c}$$

$\eta = e^{-\phi}N$ and $\phi = \exp\,(ikR\int_o^t U(t')dt')$. Thus even in its simplest form, this system cannot be reduced to an independent Mathieu equation, and hence we cannot assume that the well-known results of the solution of the Mathieu equation apply here. However, the Floquet form of solution to the Mathieu equation should work for our system. Mied (1976) used Floquet theory to analyze a similarly complicated system.

Hence we assume a solution of the form

$$P = e^{\gamma\xi/2}\sum_{n=-\infty}^{\infty} C_n e^{i\mu_n\xi}e^{i(nf-\omega)t} \tag{5}$$

in (3a), where ω is an eigenvalue. This determines that

$$\mu_n^2 = \frac{B_o^2k^2}{(\omega - nf)^2 - f^2} - \frac{\gamma^2}{4}\,. \tag{6}$$

Table 1. Summary of dimensionless parameters.

δ = aspect ratio = h/L where h is the mixed layer depth and L is the horizontal scale.
σ = horizontal Ekman number = ν_H/f_oL^2 where ν_H is the horizontal eddy viscosity and f_o the Coriolis parameter.
R = Rossby number = U_o/f_oL where U_o is velocity scale of the mean flow.
$\alpha = \delta g'/Lf_o^2$ where $g' = g\Delta\rho/\rho_1$ is the reduced gravity with $\Delta\rho$ the density jump across the interface and ρ_1 the density of the mixed layer.
$B(z) = \delta N(z)/f_o$ where $N(z)$ is the Brunt-Väisälä frequency in the interior. B^2 is a Burger number.
$B_o = \delta N_o/f_o$ = value at interface, $B(-1)$.
$\xi = 1/B_o\int_{-1}^{z} B(z')dz'$ is the transformed vertical coordinate.
$\gamma = B_\xi/B$, assumed constant.
ω = complex frequency = $\omega_r + i\omega_i$, nondimensionalized by f_o^{-1}.
k = horizontal wavenumber, nondimensionalized by L^{-1}.
ϵ = parameter partitioning energy between steady and oscillating components of mean flow.
R' = modified Rossby number = $R\sqrt{(1-\epsilon)^2+\epsilon^2}$.

3. The energy flux

A radiation condition is necessary to determine the proper roots of μ_n. We need to calculate the vertical energy flux below the mixed layer. The dimensionless vertical energy flux density, averaged over one horizontal wavelength and one inertial period, is given by:

$$
\begin{aligned}
F &= \frac{kf}{4\pi^2}\int_t^{2\pi/f+t}\int_x^{2\pi/k+x} Re(w)Re(p+\alpha\eta)\,dx'\,dt' \\
&= \frac{-fe^{-2\mu_{n_i}\xi}}{8\pi B_o^2}\frac{(e^{4\pi\omega_i/f}-1)}{\omega_i}e^{2\omega_i t}\sum_{n=-\infty}^{\infty}|C_n|^2\,Re\left[(\omega-nf)\left(\mu_n - i\frac{\gamma}{2}\right)\right] \\
&\quad - \frac{fe^{2\omega_i t}}{4\pi B_o^2}(e^{4\pi\omega_i/f}-1) \\
&\quad \sum_{\substack{m,n=-\infty \\ m\neq n}}^{\infty} Re\left[\frac{C_nC_m^*(\omega-nf)}{(2\omega_i+i(n-m)f)}\left(\mu_n - i\frac{\gamma}{2}\right)e^{i(n-m)ft}e^{i(\mu_n-\mu_m^*)\xi}\right]
\end{aligned}
\tag{7}
$$

where ω_i is the imaginary part of ω, μ_{n_i} the imaginary part of μ_n, and (*) represents the complex conjugate. The last term on the right in the above vanishes for ω real. If we assume $|\omega_i| \gtrsim .1$ and that the number of the coefficients, C_n, which have significant magnitude is not too great, (which turns out to be true), then this second term will be negligible for ω complex also. Thus, to a good approximation, the energy flux is the sum of fluxes associated with each individual wave. The energy density will behave in a similar fashion.

If we assume that there is no perturbation sources below the mixed layer, then the

energy flux for each wave (each value of n in the remaining term of (7)) must be downward or zero ($F \leq 0$). We can show that this is equivalent to the condition that unstable waves ($\omega_i > 0$) decay with depth. The proper roots for μ_n to fulfill this radiation condition are found, using (7), to be:

$$\mu_n = \begin{cases} |\mu_{n_r}| \pm i|\mu_{n_i}| & \begin{matrix}\omega_i < 0 \\ \omega_i \gtrless 0\end{matrix} \quad (\omega_r - nf) \gtrless 0 \\ -[|\mu_{n_r}| \pm i|\mu_{n_i}|] & \begin{matrix}\omega_i \gtrless 0 \\ \omega_i < 0\end{matrix} \quad (\omega_r - nf) < 0 \end{cases}, \tag{8}$$

where $|\mu_{n_r}|, |\mu_{n_i}|$ are the absolute values of the real and imaginary parts of μ_n and $\omega = \omega_r + i\omega_i$.

4. The infinite matrix

Using (5) in (3b), we find $\tilde{\eta}$ in terms of C_n so that $\tilde{p}_o$ can then be found in terms of C_n from (5) for $\xi = 0$. Then $\tilde{u}$ can be eliminated in (2a) in favor of $\tilde{\eta}$ using (2b), and finally $\tilde{\eta}$ and $\tilde{p}_o$ can be eliminated in (2a) in terms of the series yielding:

$$\sum_{n=-\infty}^{\infty} C_n e^{inft} \left\{ \left(\mu_n - i\frac{\gamma}{2}\right)[kRU - \omega + nf)(f^2 - Q_n^2 + ikRU_t) + 2ikRU_t Q_n + \alpha k^2 Q_n + kRU_{tt}] - ik^2 B_o^2 Q_n \right\} = 0, \tag{9}$$

where $Q_n = kRU - \omega + nf - i\sigma k^2$.

If we now express U in (9) in terms of exponentials from (1b) and then equate coefficients of e^{inft} to zero, we obtain the doubly infinite, banded matrix system to solve:

$$\begin{bmatrix} \cdot & \cdot & \cdot & \cdot & \cdot & \cdot & \cdot & & \\ {}_3A_{-4} & {}_2A_{-3} & {}_1A_{-2} & {}_0A_{-1} & {}_{-1}A_0 & {}_{-2}A_1 & {}_{-3}A_2 & & 0 \\ & {}_3A_{-3} & {}_2A_{-2} & {}_1A_{-1} & {}_0A_0 & {}_{-1}A_1 & {}_{-2}A_2 & {}_{-3}A_3 & \\ & & {}_3A_{-2} & {}_2A_{-1} & {}_1A_0 & {}_0A_1 & {}_{-1}A_2 & {}_{-2}A_3 & {}_{-3}A_4 \\ 0 & & \cdot & \cdot & \cdot & \cdot & \cdot & \cdot & \cdot \\ & & & \cdot & \cdot & \cdot & \cdot & \cdot & \cdot \end{bmatrix} \begin{bmatrix} \cdot \\ \cdot \\ C_{-2} \\ C_{-1} \\ C_0 \\ C_1 \\ C_2 \\ \cdot \\ \cdot \end{bmatrix} = \begin{bmatrix} \cdot \\ \cdot \\ 0 \\ 0 \\ 0 \\ 0 \\ 0 \\ \cdot \\ \cdot \end{bmatrix} \tag{10}$$

where

$$
\begin{aligned}
{}_0A_n &= \left(\mu_n - \frac{i\gamma}{2}\right)\left[\lambda_n\left(f^2 - \overline{Q}_n^2 - \frac{1}{2}\beta^2\right) - \beta^2\overline{Q}_n + \alpha k^2\overline{Q}_n\right] - ik^2B_o^2\overline{Q}_n,\\
{}_{\pm 1}A_n &= \left\{\frac{i\beta}{2}\left(\mu_n - \frac{i\gamma}{2}\right)\left[\lambda_n(f \pm 2\overline{Q}_n) \pm \left(\overline{Q}_n^2 + \frac{3}{4}\beta^2\right)\right.\right.\\
&\qquad \left.\left. \mp \alpha k^2 + 2f\overline{Q}_n\right] \mp \frac{\beta}{2}k^2B_o^2\right\} e^{\mp i\theta}\\
{}_{\pm 2}A_n &= \frac{\beta^2}{4}\left(\mu_n - \frac{i\gamma}{2}\right)[\lambda_n \pm 3f + 2\overline{Q}_n]\, e^{\mp 2i\theta}\\
{}_{\pm 3}A_n &= \mp \frac{i\beta^3}{8}\left(\mu_n - \frac{i\gamma}{2}\right) e^{\mp 3i\theta}
\end{aligned}
\tag{11}
$$

with $\overline{Q}_n = \lambda_n - i\sigma k^2$, $\lambda_n = kR(1 - \epsilon)\sin\theta - \omega + nf$ and $\beta = kR\epsilon$.

An analytical analysis of (10) is difficult. For $\epsilon = 0$ we have the model of (I) when the determinant of (10) is set equal to zero to yield ${}_0A_0 = 0$. We would like to know if there is also a parametric instability in the neighborhood of $\epsilon = 0$. For $\epsilon = 0$, the determinant consists only of the major diagonal, the ${}_0A_n$ terms. For given parameters there can be a possible neutral solution for a parametric instability if ${}_0A_n$ vanishes for more than one value of n. For ϵ small but greater than zero the terms of the first super- and subdiagonals of (10) would have to be included to determine if a neutral solution becomes an unstable solution.

We can show analytically that there is such a neutral solution for $\epsilon = 0$ which can be shown numerically to become unstable for $\epsilon > 0$. This solution exists only for $\alpha = \sigma = 0$ and has $\omega = f$ and $Rk = 2f$ for $n = -1$ and 0. This is a harmonic parametric instability since f is the forcing frequency. It also corresponds to a nonlinear resonant interaction of a wave triad in the mixed layer. The frequencies of the perturbation waves, given by $\omega - nf$, are $\omega_1 = 2f$ and $\omega_2 = f$ and their wavenumbers are $k_1 = k_2 = k$. If the "wave" associated with the mean flow has frequency $\omega_3 = f$ and a wavenumber $k_3 = 0$, then the three waves satisfy the resonance conditions $k_1 - k_2 = k_3$ and $\omega_1 - \omega_2 = \omega_3$ described by Phillips (1969). It is a second order interaction with the basic state.

It was found analytically to be impossible to have a subharmonic instability ($\omega = f/2$) for these conditions. Such an instability was never encountered for $\alpha, \sigma > 0$ either. Thus behavior analogous to the parametric subharmonic instability described by McComas and Bretherton (1977) for internal wave interactions does not seem to occur.

5. Numerical approach

Normally one would calculate values for ω, given the rest of the parameters (k, R, α, B_o, γ, ϵ, θ) such that the determinant of the matrix of (10) vanishes. However, a more

convenient solution results by fixing ω_i and calculating the unknowns R and ω_r, given k and the rest of the parameters from the two equations which are the real and imaginary parts of the vanishing determinant. We can then obtain stability curves $k = k(R)$ where $\omega_i = 0$ is a neutral curve. Values of k, R and ω_r at the point on the curve where R is a minimum are defined as critical values k_c, R_c and ω_c.

Solutions for $\epsilon > 0$ were found by using the known solution for $\epsilon = 0$ and gradually increasing ϵ. Details of the numerical process are given in the Appendix.

6. Numerical results and discussion

It was found much too costly to make sufficient calculations to be able to determine the general behavior of the solution throughout parameter space. So we examine the solution in what is considered a realistic region in parameter space. The extremes we considered for the parameters were: ϵ: $0 \rightarrow 1$, γ: $0 \rightarrow 2$, B_o: $0 \rightarrow 50$, α: $0 \rightarrow 50$ and k: $0 \rightarrow 10$. Even this region was too costly to examine thoroughly.

It is expected that the most unstable wave for $\epsilon \neq 1$ will be in the direction of the steady mean flow as in the $\epsilon = 0$ case. Limited calculations with varied θ were consistent with this expectation. So we set $\theta = \pi/2$ for all subsequent calculations.

For the values of the parameters initially assumed, we luckily found a solution for the neutral curve for every ϵ beginning at $\epsilon = 0$ and gradually increased to 1. This was lucky because we found later that neutral solutions do not exist for all ϵ for all values of the rest of the parameters.

To compensate for the fact that the average kinetic energy over one period of the mean flow will change with ϵ for U_o fixed, we define a modified value of R:

$$R' = R\sqrt{(1-\epsilon)^2 + \epsilon^2}, \tag{12}$$

where u from (1b) with $\theta = \pi/2$ and $v = \epsilon \sin ft$, consistent with this u, have been used. The average kinetic energy of the mean flow will then not change with ϵ with the use of this normalized Rossby number, R', and calculations with differing ϵ can be better compared.

Figure 1 shows the stable and unstable regions in (ϵ, k) space for $\alpha = .28$, $B_o = 3.33$ and $\gamma = 1$. For any value of ϵ the unstable region lies within the range of k for the neutral stability curve in (R', k) space. We see that for this case there exists a neutral stability solution for all realizable ϵ. The curve shown is the value of the critical value of k (k_c) as a function of ϵ. The numbers above and below the curve are respectively the values of R' and ω_r at the critical point (R'_c, ω_c). The curve is not continuous because there can exist multiple values of k on the neutral curve where R' is a relative minimum for $\epsilon > 0$ in (R', k) space. As ϵ changes, differing relative minima at differing values of k become the absolute minimum for $R'(R'_c)$ causing the jump in k_c. Multiple relative minima in (R', k) space can be seen in Figure 3.

Figure 2 has the same conditions as for Figure 1 except γ is increased to 2. Here we see that neither a neutral solution nor an instability exist for all ϵ.

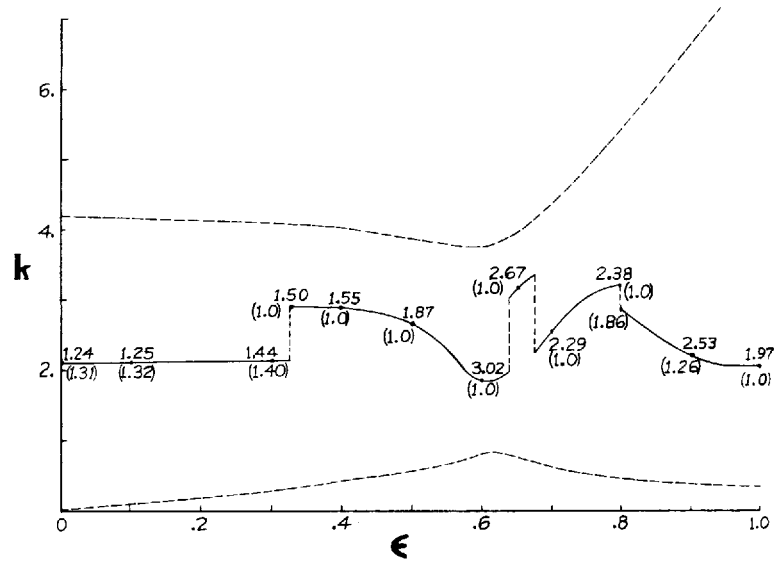

Figure 1. Stable (outside dashed lines) and unstable (inside dashed lines) regions in (ϵ, k) space for $\alpha = .28$, $B_0 = 3.33$ and $\gamma = 1$. Solid curve is k_c vs. ϵ with the numbers above being the values of R_c' and those below the values of ω_c.

We know that for $\epsilon = 0$ we have only the parallel flow type of instability. For the conditions of Figures 1 and 2 the critical point seems to be dominated by this instability for $\epsilon < .33$. If we assume that the parametric instability is dominant wherever ω_c is exactly f, then it seems to dominate for $.33 < \epsilon < .78$. For $\epsilon < .33$ there exists a local minimum of R with $\omega_r = f$, and for $\epsilon > .33$ there exists a local minimum for $\omega_r \neq f$. But neither are an absolute minimum. For $\epsilon > .78$ the parallel flow instability seems to re-emerge and then merge continuously into the parametric as $\epsilon \longrightarrow 1$.

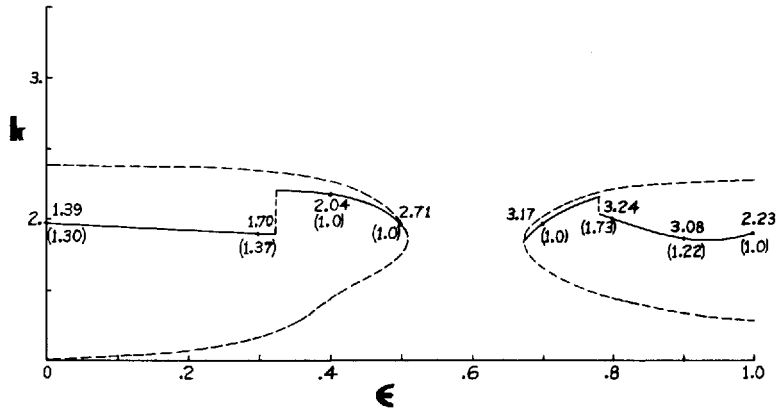

Figure 2. Same as Figure 1 except $\gamma = 2$.

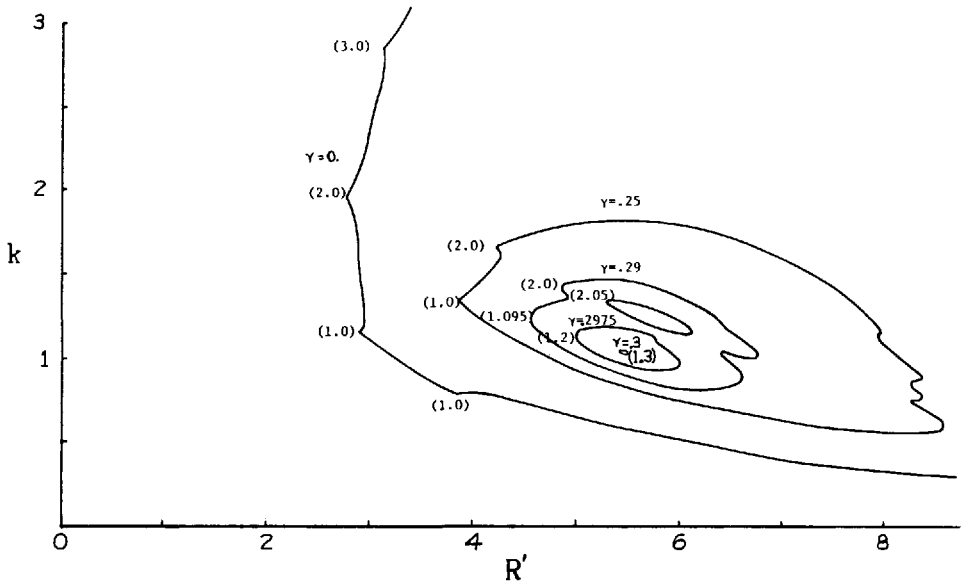

Figure 3. Neutral stability curves in (R', k) space for various values of γ. The number in parentheses is the frequency at the corresponding relative minimum in R'. $\alpha = .5$, $B_o = 1.0$ and $\epsilon = .4$.

Of importance in (I) was the result that there can be no instability unless $B_o^2 > 2\gamma f\sigma$. This means that as the stability of density stratification beneath the mixed layer increases the perturbations become more unstable.

Figure 3 illustrates that this can occur also for $\epsilon > 0$ though we cannot analytically derive definite bounds as we could for $\epsilon = 0$. On this figure are plotted neutral stability curves on the (R', k) plane for various increasing values of γ from $\gamma = 0$ for $\epsilon = .4$, $\alpha = .5$ and $B_o = 1.0$. We see that the unstable region disappears for $\gamma > .3$, a value considerably less than .5 predicted for $\epsilon = 0$.

Figure 3 shows some typical shapes for the unstable region for $\epsilon > 0$. The critical point will be the point of the absolute minimum value of R' on any curve. We see that there can be more than one relative minimum of R' for a given curve, as noted in the discussion of Figure 1. As γ approaches .3 we see that the unstable region actually separates in two parts. Each part then disappears as γ increases past .3.

The small numbers along the curves are the relative values for ω_r. The solutions for ω are not unique for $\epsilon > 0$ since any integral multiple of f can be added to it. The frequency $\omega_r - nf$ is associated with the coefficient C_n. The figure shows that at least for this value of ϵ, the critical point is likely to be exactly at the inertial frequency and be very sharply defined. Figures 1 and 2 seem to indicate that the critical frequency is likely to be exactly inertial when ϵ is such that $.3 \lesssim \epsilon \lesssim .8$ and $\epsilon \to 1$.

The set of coefficients $\{C_n\}$ for $\tilde{P}$ of (5) must be calculated. However, the

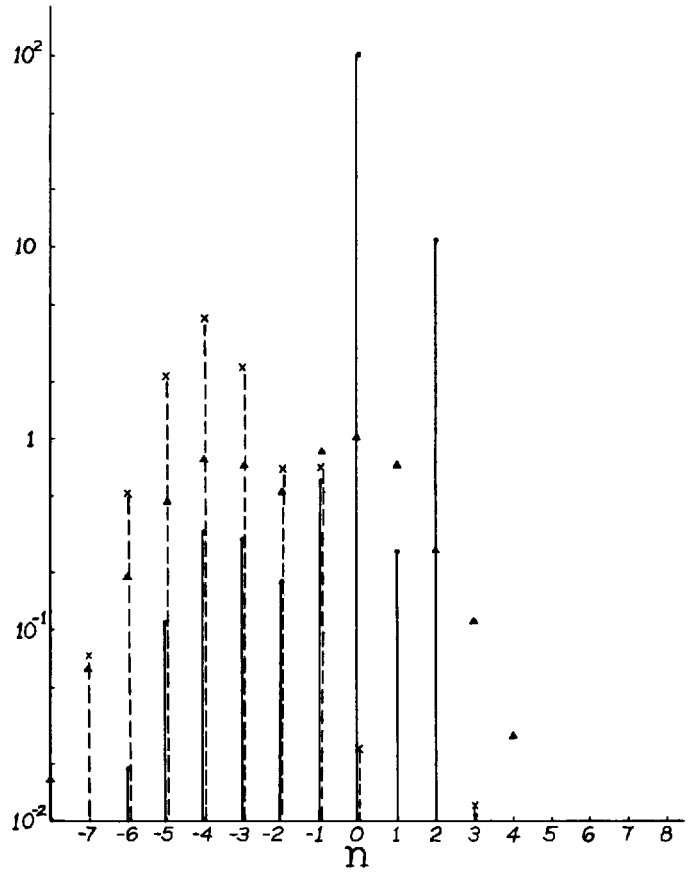

Figure 4. Values of the coefficients $|N_n|$, ▲, the energy density, •, and the energy flux density, x, versus n for $B_o = 1.$, $\alpha = .5$, $\gamma = 0$, $\epsilon = .5$, $k = 1.8$, $R' = 3.23$ and $\omega = 1.0013 + i.005$. The frequency corresponding to each n is $\omega_r - nf$.

normalization of the elements of the matrix (11) made it easier to calculate the set $\{N_n\}$ where $N_n = (\gamma/2 + i\mu_n)C_n$ for the interface displacement,

$$\tilde{\eta} = 1/B_o^2 \sum_{-\infty}^{\infty} N_n e^{-i(\omega - nf)t}$$

from (3b). The energy flux density at $\xi = 0$ for each wave can be calculated from the non-negligible first term of (7). A similar calculation for the energy density just below the interface, averaged over one wavelength and one inertial period, can also be made. These quantities are plotted for the first few terms of the sum on Figures 4, 5, 6 and 8. $|N_n|$ and the energy density are measured relative to arbitrary values for $n = 0$, 1.0 and 100., respectively.

Figures 4 and 5 are typical. The parameters for each are the same except $\epsilon = .5$ for

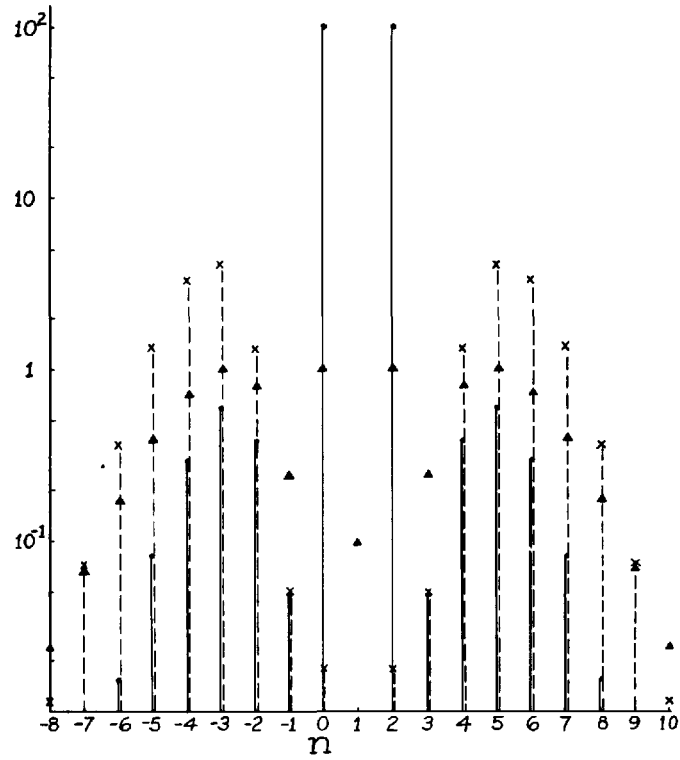

Figure 5. Same as Figure 4 but for $\epsilon = 1.$, $k = 2.06$, $R' = 3.54$ and $\omega = 1.0 + i.005$.

the former and 1.0 for the latter. Each is calculated just on the unstable side of the critical point on the neutral curve where in these cases ω_c is essentially inertial. The frequency for the nth wave is $\omega_r - nf$ so that the $n = 0$ wave has frequency $\omega_r \simeq f$. The energy flux for the 0th wave is relatively negligible but the energy density is relatively the largest as expected for a wave at almost exactly the inertial frequency. Because of division by a factor $(\omega_r - nf)^2 - f^2$, the $n = 0$ and $n = 2$ terms would be the only ones to have a nonzero relative energy density for $\omega_r = f$. The absolute values of N_n, however, are significant for $|n| \gtrsim 8$ for Figure 4 and $|n| \gtrsim 10$ for Figure 5. Figure 4 shows the dominance of $n \gtrsim 0$ corresponding to waves traveling in the direction of the steady mean. Figure 5 shows the expected symmetry about $n = 1$ for $\epsilon = 1$ where there is no steady mean flow and hence no preferred direction. It also illustrates how fast the coefficients decrease with $|n|$ even for $\epsilon = 1$.

Figure 6 shows the coefficients at the critical point for the $\gamma = .29$ curve of Figure 3. Here $\omega_r \neq f$ but is a near-inertial value of 1.095 and the energy flux for the wave at this frequency is not negligible. This illustrates the typical character of the radiation when ω is near-inertial and ϵ is sufficiently large. There can be many values of n where N_n is significant but few where the energy density is significant. The largest value of the

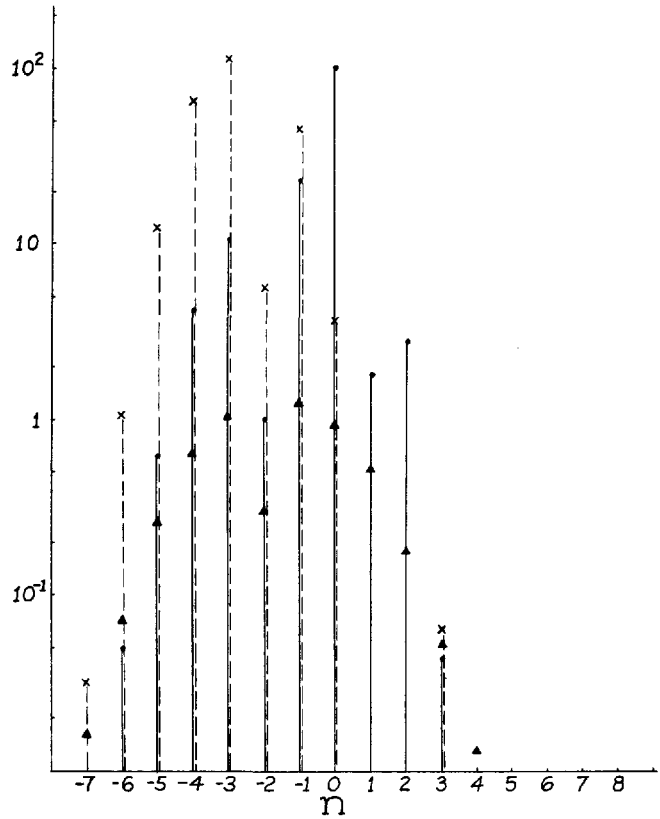

Figure 6. Same as Figure 4 but for $\gamma = .29$, $\epsilon = .4$, $k = 1.2$, $R' = 5.00$ and $\omega = 1.095$.

energy density is at the frequency ω_r ($n = 0$), but the largest energy flux will be at a higher frequency $\omega_r - nf$ with $n < 0$ for $\epsilon < 1$. For the conditions of Figure 6 the largest flux occurs at $n = -3$, which is a frequency 4.095, with a flux about 30 times greater than for $n = 0$. The fluxes at $n = -4$ and -1 are also quite significant. These fluxes are larger than for $n = 0$ because the group velocity increases with frequency and so with $|n|$. But ultimately the energy density decreases sufficiently with $|n|$ to force the flux to also decrease with $|n|$.

We conclude that for a sufficient value of ϵ, if there is an instability with ω_r near-inertial, the energy observed immediately beneath the mixed layer will be predominantly at ω_r but the energy flux will be at higher frequencies, $\omega_r + |n|f$. Titov (1973) claims to have seen spectral peaks not only near the inertial frequency but also at approximately integral multiples of inertial in the Mediterranean and Black Seas and the Atlantic and Indian Oceans. This has not seemed to be a general observation. However, recently Pinkel (1983) has interpreted data from FLIP as showing significant energy near integral multiples of the inertial frequency.

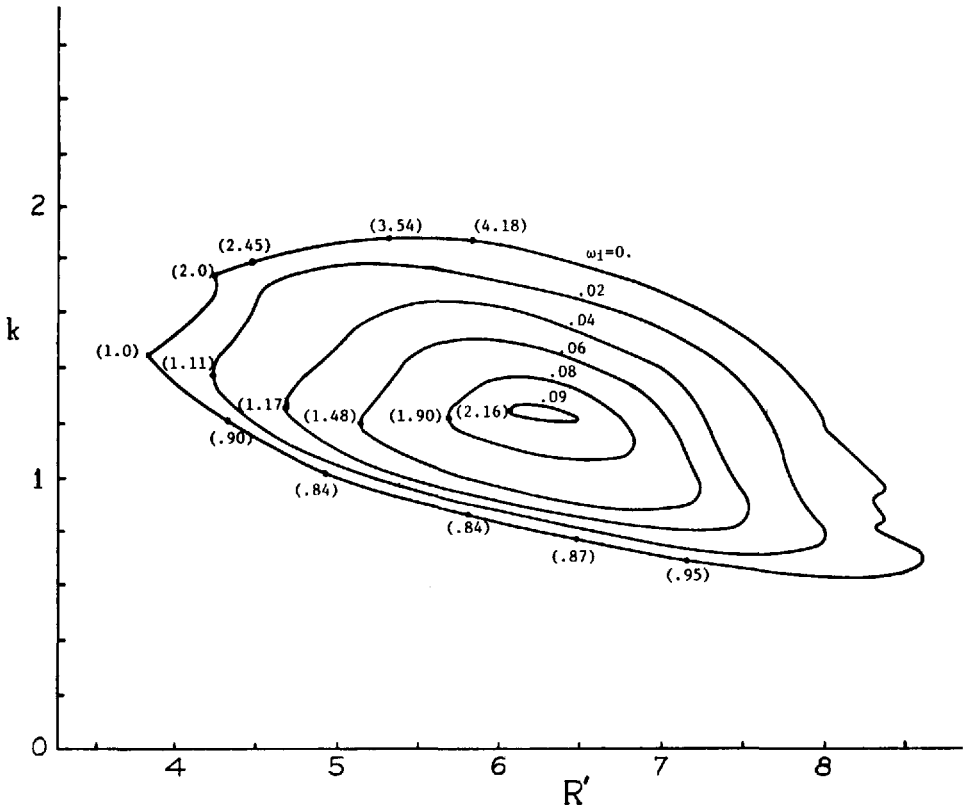

Figure 7. Typical curves in (R', k) space for various constant unstable values of ω_i. The numbers in parentheses are frequencies ω_r. $\alpha = .5$, $B_o = 1.0$, $\gamma = .25$ and $\epsilon = .4$.

Clearly the above is dependent on ϵ. As $\epsilon \to 0$ all the coefficients except for $n = 0$ go to zero. The limited calculations made indicate the number of significant coefficients increases as ϵ increases as expected. However, not enough calculations were made to determine how variations of the other parameters affect this. Figure 5, for $\epsilon = 1$, indicates this number of significant coefficients is limited.

For $\epsilon > 0$ it seems typical to have a critical point on a neutral curve where $\omega = f$. Waves at a frequency exactly f will not propagate vertically. However, typically the critical frequency increases as the critical value of R is exceeded and one moves into the unstable region. This is illustrated in Figure 7 where curves of constant values of the imaginary part of ω, ω_i, are drawn for the $\gamma = .25$ case of Figure 3. If R' is increased from the critical value of 3.87 to 4.24, the most unstable solution has $\omega_i = .02$, $k = 1.31$ and $\omega_r = 1.11$. Figure 8 shows the normalized values for $|N_n|$ at this point. The results are similar to Figure 6 with again the energy concentrated at $n = 0$ and the flux concentrated about $n = -3$.

For the conditions of Figure 7, the most unstable solution has $\omega_i \simeq .095$, $k \simeq 1.2$ and

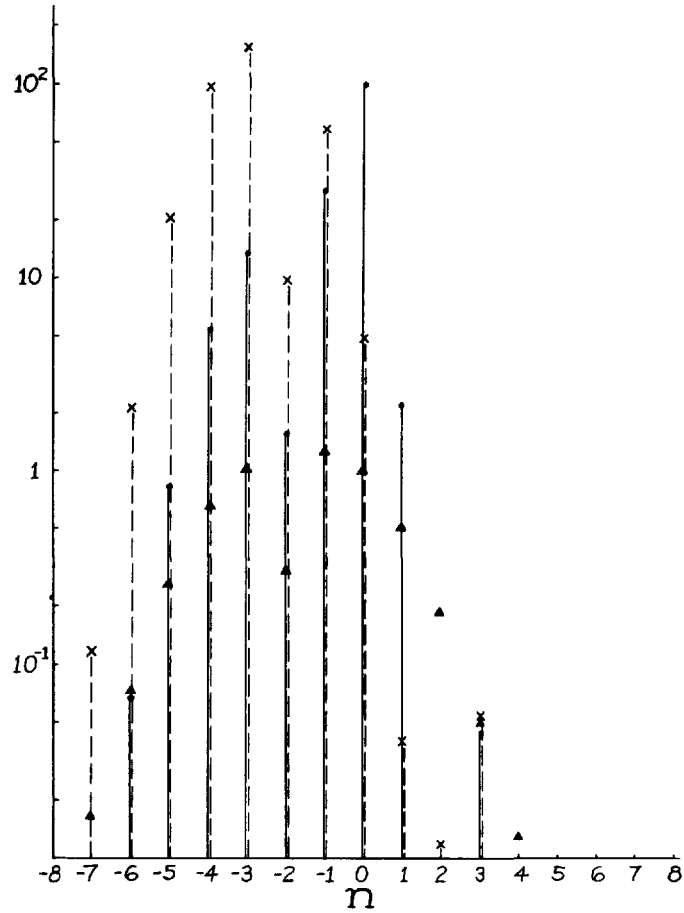

Figure 8. Same as Figure 4 but for $\gamma = .25$, $\epsilon = .4$, $k = 1.31$, $R' = 4.24$ and $\omega = 1.109 + i.02$.

$\omega_r \simeq 1.2$ at $R' \simeq 6.3$. At midlatitudes this would imply a growth by a factor e in about 2 days. As R' is increased to 6.3, the value of ω_r at the most unstable point for a given R' will go through values which will not be near-inertial. So near-neutral unstable solutions are likely to be dominated by a near-inertial frequency while the more unstable solutions may not be near-inertial.

The values of the parameters used so far should be nominally realistic. Realistic parameters can be estimated from actual data. From Site D data (Pollard, 1980), we estimate that $N_o/f_o \simeq 400$, $h \simeq 25$ m, $\gamma \simeq 1$ and $g' \simeq .1$ cm/sec^2. What we know least is ν_H. So we plot for various values of ϵ the critical values for R', ω, and k versus $L = \sqrt{\nu_H/f_o}$. These are shown on Figures 9, 10, and 11. (Figures 1 and 2 correspond to these same values of N_o/f_o, g' and h with $L = 3$ km.)

For $\epsilon = 0$, the maximum value for L for which there can be an instability can be

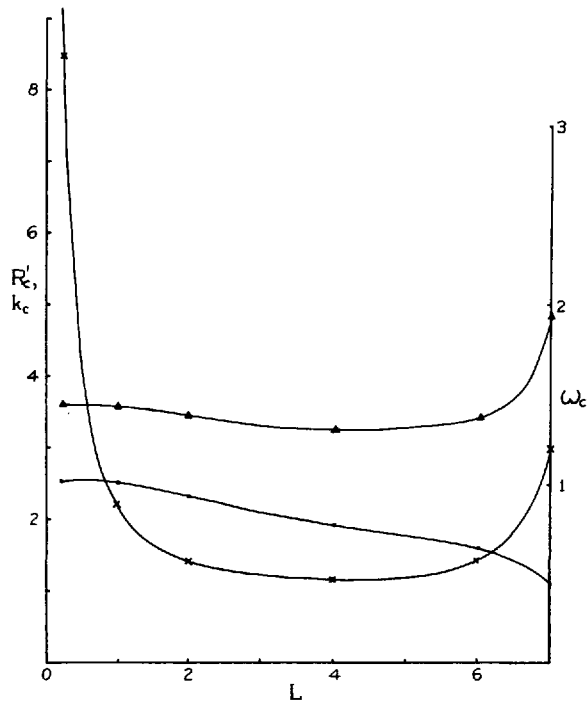

Figure 9. $R_c'(x)$, $k_c(\cdot)$, $\omega_c(\blacktriangle)$ vs. $L = \sqrt{\nu_H/f_o}$(km) for $\epsilon = 0$, $\gamma = 1$, $g' = .1$ cm/sec^2, $h = 25$ m, $N_o/f_o = 400$ and $\omega_i = 0$.

calculated from the inequality derived in (I). This is shown in Figure 9 where the maximum L is about 7.1 km. In the interval of L from .2 to 7.1 km. the minimum value of ω_c is 1.3 which is about out of the near-inertial range.

In contrast, for $\epsilon = .5$ shown on Figure 10, ω_c is exactly 1 for the whole interval of L shown. The maximum value of L is about 5 km which cannot be derived analytically. The maximum value of L is less than that for $\epsilon = 0$ and the value of R_c' is greater for most values of L.

Figure 11 for $\epsilon = 1$ has discontinuities like Figures 1 and 2 for the same reason. Differing relative critical points become absolute critical points as L is increasing. Figure 12 illustrates an unusual example of this. As L increases from .2 to .7 km an "island" of instability is gradually pinched off the "mainland" of the unstable region. The absolute critical point is on the left side of the "island." As L is increased to .75 km the "island" disappears and the absolute critical point becomes the relative critical point at about $k = 4.3$ of Figure 12. As L is increased more, the relative critical point at about $k = 1.6$ on Figure 12 gradually draws even with the one at the larger value of k for L about 1.5 km. Thereafter this critical point remains the absolute critical point.

The value of ω_c is 1 for all L and is not shown on Figure 11. The maximum possible

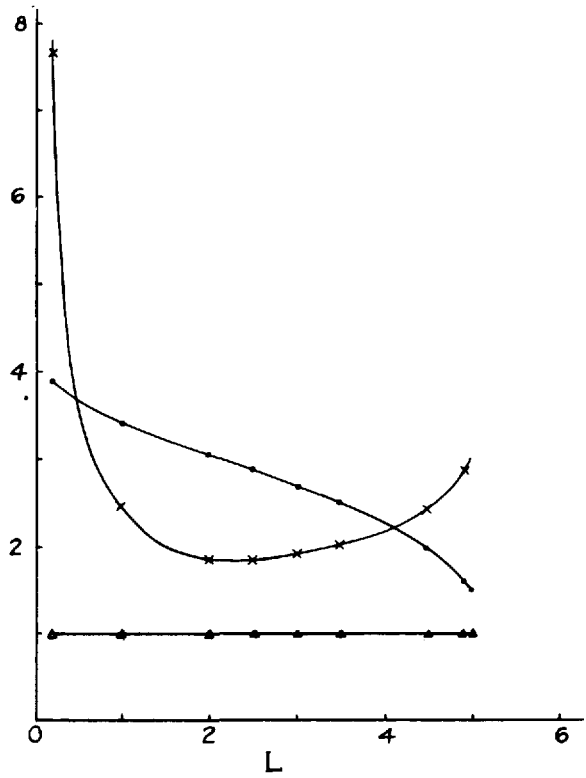

Figure 10. R_c' (x), k_c (·) and ω_c (▲) vs. L(km) for the same conditions as Figure 9 except ϵ = .5.

value for L is about 6.2 km. and is greater than that for ϵ = .5 and R_c' is generally comparable to that for ϵ = .5 for most values of L shown.

The flow scenarios in (I) for ϵ = 0, the "increasing flowrate" and "increasing depth" instabilities, will not be examined here because the cost of computation is prohibitive. We can look at some data for the mean flow to see under what circumstances the flow could be unstable. From the data of Pollard, the value of ϵ varies from about .3 to .8. The largest mean flow in the data has ϵ about .6 and U_o about 90 cm/sec. For N_o/f_o = 400, γ = 1, and h = 25 m, $f_o = .9 \cdot 10^{-4}$ sec^{-1} and L = 3 km. Figure 1 indicates $R_c' \simeq$ 3.0, $k_c \simeq 1.85$, $\omega_c = 1.0$ so that $U_o = R_c' f_o L/\sqrt{(1-\epsilon)^2 + \epsilon^2} \simeq 110$ cm/sec and the wavelength $L_x = 2\pi L/k_c \simeq 10$ km. So for this value of $L = \sqrt{\nu_H/f_o}$ we would not expect an instability. If L is chosen to be 2.5 km, the critical flow is about 90 cm/sec. Since U_o varies linearly with L and R_c' does not change much until L becomes sufficiently small, U_o at the critical value continues to decrease until a minimum is reached. So an instability is possible depending on L.

Of the figures for varying L, Figure 10 for ϵ = .5 is the most realistic. At the maximum L at which there can be an instability, L = 5 km, the value of U_o is about 200

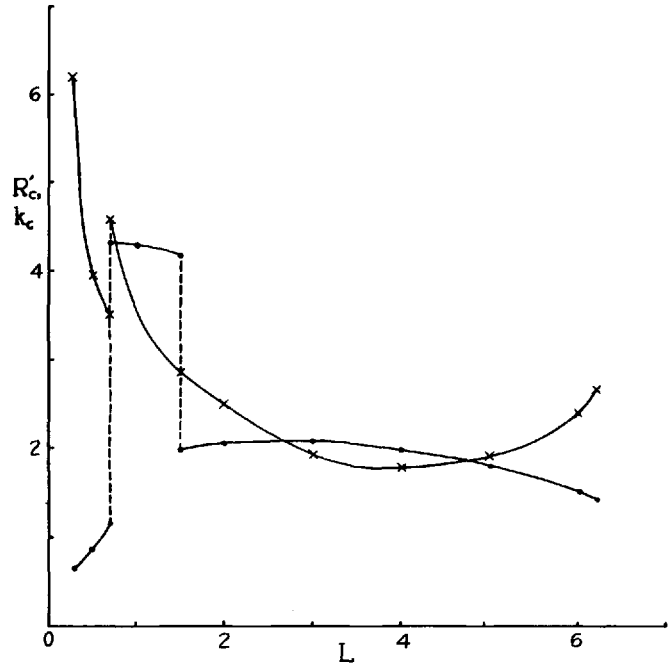

Figure 11. Same as Figure 10 except $\epsilon = 1.0$ and $\omega_c = 1.0$ for all L.

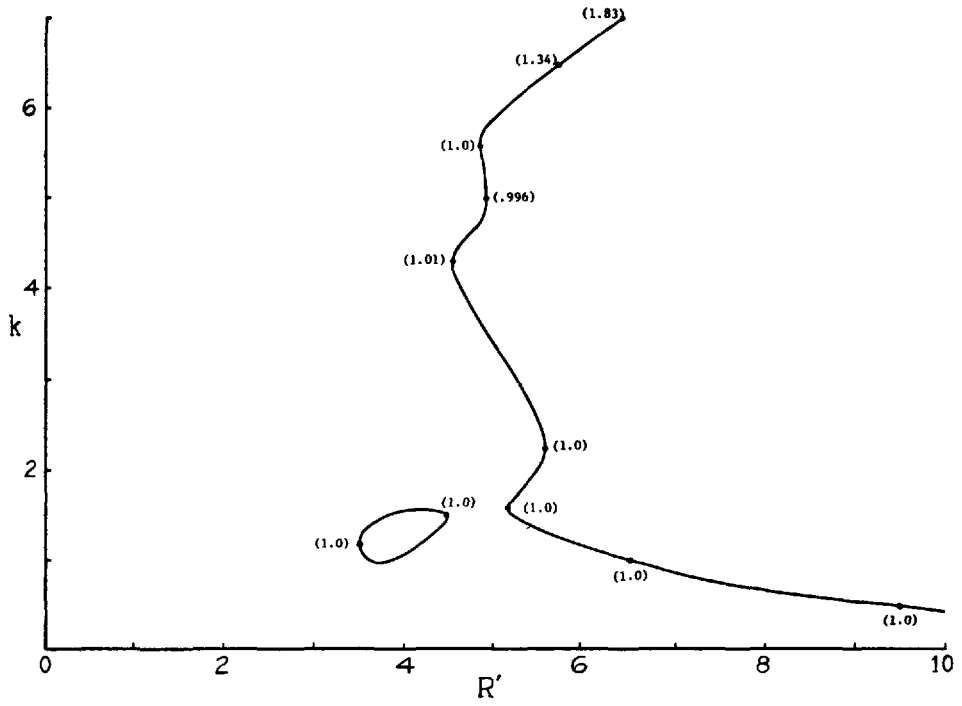

Figure 12. Neutral stability curve for the conditions of Figure 11 for $L = .7$ km. The numbers in parentheses are frequencies, ω_r.

cm/sec which is unrealistically large. The value of U_o is a minimum of about 20 cm/sec at about $L = .7$ km where the wavelength, L_x, is about 1.2 km. So here the flow is easily obtained but the wavelength would seem unreasonably small. The limited amount of data indicates that L_x should be 0 (10 km) (Sanford, 1975; Pinkel, 1983 for example). So assuming that $U_o \gtrsim 100$ cm/sec is realistic, then L on Figure 6 cannot be any larger than about 4 which corresponds to a wavelength of about 10 km. If $L_x \gtrsim 5$ km. is realistic, then L cannot be any smaller than about 2 km. So to have instability at these conditions, the horizontal eddy viscosity must be such that $4 \cdot 10^6$ cm^2/sec $\lesssim \nu_H \lesssim 16 \cdot 10^6$ cm^2/sec, a somewhat limited range. This range can be expanded by varying the parameters, an increase in h or a decrease in g', for example.

7. Summary of results

Based on the limited calculations shown in the figures and a few not shown, the more important results are:

1. The solution seems to behave in the same manner as (I) ($\epsilon = 0$) with respect to the parameters α, B_o and γ. That is the value for R_c increases (higher stability) and k_c decreases as B_o decreases, γ increases or α increases. Thus, as with (I), a more stable density stratification produces less flow stability. (Based on Figure 3 and calculations not shown.)
2. The frequency at the critical point, ω_c, is much more likely to be near-inertial for $\epsilon \gtrsim .3$ than for $\epsilon = 0$. (Figs. 1, 2, 9, 10, 11.)
3. The critical frequency increases as R' is increased from R'_c. This allows energy originally at a frequency that is exactly inertial on the neutral curve to vertically propagate at a near-inertial frequency. The energy of the resulting wave is concentrated at the near-inertial frequency though there can be significant components which are integral multiples of the inertial frequency above the near-inertial frequency. The energy flux is concentrated in these higher frequencies and the flux associated with the near-inertial frequency is insignificant in comparison (Fig. 11, Fig. 8).
4. The growth of an unstable wave is limited as in (I). The frequency at the point of greatest growth is not necessarily going to be near-inertial. (Fig. 7).
5. As in (I) the magnitude of ν_H, which is unknown, will be significant in determining whether the flow can become unstable. For the data considered, $\nu_H = 0(10^7$ cm^2/sec) seems to be necessary. This restriction on ν_H can be relaxed with various changes in the values of the parameters.

8. Conclusions

The analysis of this model with the realistic addition of inertial oscillations in the mean flow reinforces my contention that this instability can be a source of downward propagating near-inertial motion. Not unexpectedly, if there is an instability, this model will more likely have perturbations with near-inertial frequency than the steady mean flow model of (I).

Also, as might be expected from the nature of a parametric instability, frequencies that are nearly integral multiples of the inertial frequency can be significant. The observation of such would be evidence of the existence of the instability. However, the instability can still be occurring while the amplitudes of super-inertial frequencies are not significant enough to detect. Interestingly, though the super-inertial waves would be difficult to detect, they would constitute the greatest energy sink of the steady state from this instability mechanism.

This model is mathematically involved but still rather crude physically. The velocity of the real mixed layer has some shear especially in the direction normal to the direction of the transport. More importantly the problem of finding the amplitude of the energy flux of the perturbation from the mixed layer should be addressed to see if it is a significant energy sink for the mixed layer energy budget.

Acknowledgments. The research was supported by the National Science Foundation, grant number OCE-8006048.

APPENDIX

It makes sense to utilize the solution for the $\epsilon = 0$ case already known, to gradually increase ϵ from zero and look for a solution in the neighborhood of a previous solution. It then makes sense to assume that the dominant coefficient is ${}_0A_0$ and to rearrange the matrix in (10) to obtain a semi-infinite banded matrix system to solve:

$$\begin{bmatrix} {}_0A_0 & {}_{-1}A_1 & {}_1A_{-1} & {}_{-2}A_2 & {}_2A_{-2} & {}_{-2}A_3 & {}_3A_{-3} & 0 \\ {}_1A_0 & {}_0A_1 & {}_2A_{-1} & {}_{-1}A_2 & {}_3A_{-2} & {}_{-2}A_3 & 0 & {}_{-3}A_4 \\ {}_{-1}A_0 & {}_{-2}A_1 & \cdot & \cdot & \cdot & \cdot & \cdot & \cdot \\ {}_2A_0 & {}_1A_1 & \cdot & \cdot & \cdot & \cdot & \cdot & \cdot \\ {}_{-2}A_0 & {}_{-3}A_1 & \cdot & \cdot & \cdot & \cdot & \cdot & \cdot \\ {}_3A_0 & {}_2A_1 & \cdot & & & & & \\ {}_{-3}A_0 & 0 & \cdot & & & & & \\ & {}_3A_1 & \cdot & & & & & \\ 0 & & \cdot & & & & & \end{bmatrix} \begin{bmatrix} C_0 \\ C_1 \\ C_{-1} \\ C_2 \\ C_{-2} \\ \cdot \\ \cdot \\ \cdot \\ \cdot \end{bmatrix} = \begin{bmatrix} 0 \\ 0 \\ 0 \\ 0 \\ 0 \\ \cdot \\ \cdot \\ \cdot \\ \cdot \end{bmatrix}$$

Not much is known about such systems (Smith pers. comm.). The only known method to find a solution is truncation (e.g., Mied, 1976), where one decides that an accurate value of ω is obtained when an increase in the order of the determinant changes the value of ω only negligibly and the coefficients, C_n, decay toward zero for increasing $|n|$. Rather than calculate complex ω, we calculate stability curves $k = k(R)$. $Im(\omega)$ is fixed ($Im(\omega) = 0$ for the neutral curve), and we calculate the two unknowns $Re(\omega)$ and R, given k and the rest of the parameters, from the two equations which are the real and imaginary parts of the determinant set to zero. We use a two

dimensional Newton's method scheme to find these values, using Gauss elimination to evaluate the determinant. The order of the determinant necessary for reasonable accuracy ranges from 1 for $\epsilon = 0$ to around 50 for $\epsilon = 1$. Reasonable accuracy was arbitrarily chosen to be a relative change of the calculated values of less than about 10^{-3} for an increase in the order of the determinant of 5.

REFERENCES

Kelly, R. E. 1965. The stability of an unsteady Kelvin-Helmholtz flow. J. Fluid Mech., *22,* 547–560.

Kroll, John. 1982. An unstable uniform slab model of the mixed layer as a source of downward propagating near-inertial motion. Part I: steady mean flow. J. Mar. Res., *40,* 1013–1033.

McComas, C. H. and F. P. Bretherton. 1977. Resonant interaction of oceanic internal waves. J. Geophys. Res., *82,* 1397–1412.

Mied, Richard P. 1976. The occurrence of parametric instabilities in finite amplitude internal gravity waves. J. Fluid Mech., *78,* 763–784.

Orlanski, Isidoro. 1973. Trapeze instability as a source of internal gravity waves. Part I. J. Atm. Sci., *30,* 1007–1016.

Phillips, O. M. 1969. The Dynamics of the Upper Ocean. Cambridge University Press.

Pinkel, R. 1983. Doppler sonar observations of internal waves: wave-field structure. J. Phys. Oceanogr., *13,* 804–815.

Pollard, R. T. 1980. Properties of near-surface inertial oscillations. J. Phys. Oceanogr., *10,* 385–398.

Sanford, T. B. 1975. Observations of the vertical structure of internal waves. J. Geophys. Res., *80,* 3861–3871.

Smith, Philip W., Professor of Mathematical Sciences, Old Dominion University, Norfolk, Virginia, personal communication.

Titov, V. B. 1973. Some distinctive features of mesoscale motions in the sea. Oceanology, *13,* 794–798.

Received: *12 January, 1983;* revised: *7 November, 1983.*